Dual Neural Network Control of a Hybrid FES Cycling System

Glen R. Merritt, Saiedeh Akbari, Christian A. Cousin, Hwan-Sik Yoon*

***Abstract*—Hybrid FES cycling is a method to rehabilitate people with neurological conditions when they are not in and of themselves capable of fully controlling their extremities. To ensure smooth cycling and adequate stimulation to accomplish the rehabilitation task, admittance control is applied between the human and the robotic cycle. The cycle motor is actuated by a dual neural network control structure with an additional robust element tracking the admittance trajectory, while muscles are stimulated with a simple saturated robust controller. The dual neural network structure allows adaptation to separable functions of the dynamic system, in addition to shared adaptation through the admittance filter. A Lyapunov analysis shows that the admittance tracking controller is globally exponentially stable. A passivity analysis shows that the admittance system and cadence tracking error are output strictly passive. A combined analysis shows that the total system is passive. Experiments are performed on eight participants without neurological conditions, on twelve differing protocols including a robust controller for comparison, the addition of noise, and the addition or lack of stimulation. One participant with a neurological condition was evaluated on three different protocols, including a robust controller, a neural network controller and a game-like mode where the participant was asked to track the trajectory as it appeared on a screen. Statistical analysis of the experiments show that the standard deviation of the tracking error is significantly improved with the adaptive dual neural network control addition when compared to the robust controller.**

***Index Terms*—Functional electrical stimulation (FES), exoskeletons, Lyapunov, nonlinear, neural network, admittance, passivity, rehabilitation**

I. Introduction

For millions of Americans, there exist sustained neurological injuries such as stroke, traumatic spinal cord injury, and traumatic spinal cord injury that can negatively impact their ability to live their lives comfortably [1], in addition to an increased risk of future degeneration, secondary health impairments, and death [2]. For people who live with such neurological conditions, there is an increasing need for rehabilitation options that allow them to recover functionality and regain their independence and health [3]. Such rehabilitation could lead to improved overall metabolic health and generally improved quality of life. Rehabilitation in general is a key strategy for providing people with neurological conditions a method to reclaim their life, and two strategies: FES and robotic assistance coupled together offset the weaknesses of each individually in therapy.

G. R. Merritt, S. Akbari, C. A. Cousin, and H. S. Yoon are with the Department of Mechanical Engineering, University of Alabama, Tuscaloosa, AL 35401,USA Email: {gmerritt, sakbari}@crimson.ua.edu,{cacousin, hyoon}@eng.ua.edu

Functional electrical stimulation (FES) has proven benefits in therapeutic practices including improved bone mineral density, cardiovascular parameters, and preservation of muscle mass [4]–[6], and has been utilized in many previous studies to facilitate a paradigm where the human musculoskeletal system is idealized as a Lagrangian system, often with uncertain delays, unknown control effectiveness, and limitations in the domain in which control can be applied [7]. These considerations imply that FES alone is insufficient for the rehabilitation paradigm and cannot by itself be used to accurately control human muscle. FES is inferior to volitional muscle contractions [8], further suggesting that, when capable, the rehabilitation task should be done volitionally in addition to with electrical stimulation.

Human robotic interaction necessitates that robots be compliant and safe when in contact with a human rider or interaction subject [9], [10]. This asks the robot to be able to operate in a different domain than the traditional position and kinematic relationships that are central to industrial and autonomous systems. Rehabilitative robotics in particular requires interacting with dynamics that are not even necessarily within the human participant's control as is the case for those with SCI injuries or other neurological conditions [11]–[13]. In particular, the coupled exoskeleton approach [14], [15] presents a framework for combing the human and the robotic control into one single system and having the designed system achieve the desired control trajectory i.e. rehabilitative task. The difficulty therein lies in accommodating the eccentricities of controlling the human body externally, which constitutes a nonlinear, switched, and evolving dynamics problem.

Coupled systems that compensate for these weaknesses and allow asymptotic convergence are the next step in addressing the human-robot interaction problem, and allowing the built-in control scheme to operate in a small region around the desired trajectory, the admittance defined force field region. Admittance, the dual of impedance as formulated originally by Hogan [16], presents a method for translating this deviation into a force-based interaction model. Admittance control then translates easily into an assist-as-needed approach [17]–[19]. Minimizing assistance allows the Neurological subject to perform the task as volitionally as possible [17], [19].

Hybrid FES cycling in particular, targets the lower limbs, which are vital to walking and standing and thus thoroughly impact the quality of life. To address the above issues, a continuous mechanical system in the form of an electric motor is used instead to track the main part of the desired trajectory, stimulation occurs while in an applicable zone, and

Fig. 1. An experimental subject seated on the cycle. Equipment includes A: Orthotic boots, B: Pedals, C: Stimulation electrodes, D: Stimulator Unit, and E: DC Motor.

an additional control system monitors the interaction between the coupled system. Previous attempts at designing a control system to facilitate coupled human-robotic interfaces have focused on a variety of control strategies such as robust sliding mode [20] and adaptive [21]. Passivity alone as control design strategy has been attempted as well [22]. Some attempts have also combined some of the previous strategies and proven the necessary conditions to induce error convergence and prove stability [23]–[25]. It is difficult with these approaches to prove global exponential stability, especially due to the existence of deadzones and unknown delays in control activation. The final step is to incorporate power tracking in the model, which is used in the admittance system indirectly [23]–[25]. Asymmetries are an outstanding issue as well, though some works seek to address them [26]. With the previous work in mind, the proposed controller consists of robust and neural network adaptive terms monitoring the force exerted by the motor, which adapts to the Lagrangian combined dynamics of the coupled mechanical system, an adaptive system for the admittance trajectory in the system, and an admittance filter which creates a aritificial soft interaction between the human and electromechanical system. The primary error system with the admittance trajectory is proven stable in the sense of Lyapunov (i.s.L), and the error system that does not include the admittance error is proven output feedback passive in the sense of Khalil (i.s.K.) [27], [28].

II. Dynamics

A. Hybrid Exoskeleton Model

Let $n \in \mathbb{N}$ denote the number of joints of the hybrid exoskeleton and let $q \in \mathbb{R}^n$, $\dot{q} \in \mathbb{R}^n$, and $\ddot{q} \in \mathbb{R}^n$ denote the measurable angles, the measurable angular velocities, and the unknown angular accelerations of the exoskeleton's joints, respectively. For the purpose of cycling the wrapped crank angle is restriced to the set $q \in \mathcal{Q} \subseteqq \mathbb{S}$where $\mathbb{S}$ is the one dimensional sphere. The dynamics of the hybrid exoskeleton can be represented by [1]

$$M(q)\ddot{q} + C(q,\dot{q})\dot{q} + G(q) + P(q,\dot{q}) + b\dot{q} + d(t) = \sum_{m\in\mathcal{M}} b_m(q,\dot{q})\sigma_m(q)u_h(t) + B_e u_e(t), \quad (1)$$

where the inertia, centripetal-Coriolis, and gravitational effects are denoted by $M : \mathbb{R}^n \to \mathbb{R}^{n\times n}$, $C : \mathbb{R}^{2n} \to \mathbb{R}^{n\times n}$, and $G : \mathbb{R}^n \to \mathbb{R}^n$, respectively. The passive viscoelastic tissue torques of the human, the friction effects of the exoskeleton, and disturbances (e.g., changes in load or muscles spasms) are denoted by $P : \mathbb{R}^{2n} \to \mathbb{R}^n$, $b \in \mathbb{R}^{n\times n}_{>0}$, and $d \in \mathbb{R}^n$, respectively. Torque supplied by the electric motor is denoted by $\tau_e : \mathbb{R}_{\geq t_0} \to \mathbb{R}^n$ and can be defined as

$$\tau_e(t) \triangleq B_e u_e(t), \quad (2)$$

where $B_e \in \mathbb{R}^{n\times n}_{>0}$ denotes the known motor control constants mapping each motor's input current to output torque and $u_e : \mathbb{R}_{\geq t_0} \to \mathbb{R}^n$ denotes the yet to be designed motor control current. The torque generated by rider's lower limb muscles is denoted by $\tau_h : \mathbb{R}^n \times \mathbb{R}^n \times \mathbb{R}_{\geq 0} \to \mathbb{R}^n$ and can be defined as

$$\tau_h(q,\dot{q},t) \triangleq B_h(q,\dot{q})\sigma_h(u_h(t))u_h(t), \quad (3)$$

where $B_h : \mathbb{R}^n \times \mathbb{R}^n \to \mathbb{R}^{n\times 2n}_{>0}$ denotes the unknown muscle control effectiveness terms mapping stimulation to joint torque[2], $\sigma_h : \mathbb{R}^n \to \{0,\ 1\}^{2n\times n}$ denotes the piecewise right-continuous matrix of switching signals for activating the rider's individual muscle groups, and $u_h : \mathbb{R}_{\geq 0} \to \mathbb{R}^n$ denotes the subsequently designed muscle control value.

B. Muscle Activation

The set of all muscles to be stimulated is given by the cartesian product $\mathcal{M} \triangleq \{R, L\} \times \{Q, H, G\}$,where R, L are the right and left sides, and Q, H, G represent the quadriceps femoris, hamstring, and gluteal muscles. The msucle control effectiveness term combining all of the groups capable of providing torque is denoted as

$$B_h \triangleq \sum_{m\in\mathcal{M}} b_m(q,\dot{q})\sigma_m(q), \quad (4)$$

where b_m is the effectiveness of a particular muscle group $m \in \mathcal{M}$ and σ_m is the switching signal turning on stimulation according to the bivalued mapping

$$\sigma_m \triangleq \begin{cases} 1 & q \in \mathcal{Q}_m \\ 0 & q \notin \mathcal{Q}_m \end{cases}, \quad (5)$$

[1]For notational brevity, all explicit dependence on time, t, within the states $q(t)$, $\dot{q}(t)$, $\ddot{q}(t)$ is suppressed.

[2]Because muscles can only exert forces/torques through contractions, a minimum of two muscles (or muscle groups) are required for bidirectional articulation for each joint. Therefore, for an n degree of freedom system, a minimum of $2n$ muscles (or muscle groups) are needed for full actuation.

where $\mathcal{Q}_m$ is the region for each group m for which it can adequately contribute to the cycling task. A more detailed description of $\mathcal{Q}_m$ is given in [29].

Property 1. The inertia matrix $M(q)$ is a symmetric, positive-definite matrix that satisfies $c_m \|\theta\|^2 \leq \theta^\top M(q)\,\theta \leq c_M \|\theta\|^2$, $\forall \theta \in \mathbb{R}^n$ where $c_m,\ c_M \in \mathbb{R}_{>0}$ are known constants and $\|\cdot\|$ denotes the Euclidean norm [30].

Property 2. The inertia and centripetal-Coriolis matrices satisfy the skew-symmetric relationship $\theta^\top \left(\dot{M}(q) - 2C(q,\dot{q})\right)\theta = 0.\ \forall \theta \in \mathbb{R}^n$ [30].

Property 3. The centripetal-Coriolis, gravity, viscoelastic tissue, friction, and disturbance terms of (1) can be upper bounded as $\|C(q,\dot{q})\|_{i\infty} \leq c_C \|\dot{q}\|$, $\|G\|_\infty \leq c_G$, $\|P\|_\infty \leq c_{P1} + c_{P2}\|\dot{q}\|$, $\|b\|_{i\infty} \leq c_b$, $\|d\|_\infty \leq c_d$ where $c_C,\ c_G,\ c_{P1},\ c_{P2},\ c_b,\ c_d \in \mathbb{R}_{>0}$ are known constants, $\|\cdot\|_\infty$ denotes the infinity-norm of a vector, and $\|\cdot\|_{i\infty}$ denotes the infinity-norm of a matrix [30], [31].

Property 4. The unknown muscle control effectiveness matrix B_h can be bounded by $B_{\underline{h}} \leq \|B_h\|_{i\infty}$ and $\|B_h\|_{i\infty} \leq B_{\overline{h}}$, where $B_{\underline{h}},\ B_{\overline{h}} \in \mathbb{R}_{>0}$ are known constants denoting the bounds of the infinity norm of B_h for all time. [31].

III. Control Development

The hybrid FES cycle, with its better understood and controllable physical aspects, handles the most difficult parts of the tracking task and allows the rider to exert maximum or necessary force in accordance with their stimulation parameters and muscular capability, and to provide challenge where possible [32]. This is synonymous with the rehabilitation objective, where it is desired for the human rider to exert force when available, but coordinating the muscular contractions with unknown dynamic parameters, switched and time-varying control effectiveness, and the possibility of voluntary contraction is difficult to achieve as a solitary position and cadence tracking objective. Admittance control instead offers an opportunity for the better understood, easier to control, and time-invariant dynamic parameters and control effectiveness of the electromechanical exoskeleton to attempt to track the cadence and position objectives, with allowance for the contribution of the rider's muscles. To this end, the error system combines the absolute tracking error with the error generated by a force admittance filter tuned by the programmer, and the admitted trajectory forms the secondary tracking objective.

The designed adaptive controller has integral terms which contribute smoothness to the tracking objective of the rider since the desired cadence and position are integral terms. This avoids large fluctuations in the desired force output from the operator's muscles which would likely lead to discomfort and early fatigue. Adaptation and robustness are instead applied to the cycle motor, so error convergence is achieved on the admittance trajectory, while sharing the adaptation to the combined system dynamics with the rider. The inertial and Coriolis components are lumped, so adaptation still applies to the physical dynamics of both subsystems, which are sufficiently static, and the admittance system accounts only for the force contribution of the rider.

A. Error System Development

Error is developed in two respects: the position error e and the error augmented by the admittance filter error[3] ξ. Both are contained within the filtered tracking errors r and ψ, which contain e and ξ, respectively. Both are developed beginning with the desired motion trajectory $q_d : \mathbb{R}_{\geq 0} \to \mathcal{Q}^n$, where the set $\mathcal{Q}^n \subseteq \mathbb{R}^n$ is selected such that all joint angles are restricted to those achievable by the cycle, and designed to be sufficiently smooth (i.e., $q_d,\ \dot{q}_d,\ \ddot{q}_d \in \mathcal{L}_\infty$) to allow adaptation by the neural networks. The position error $e : \mathbb{R}_{\geq 0} \to \mathbb{R}^n$ and filtered tracking position error $r : \mathbb{R}_{\geq 0} \to \mathbb{R}^n$ are introduced and utilized in the tracking of the desired cadence by muscular contraction as described in Section II-B. The composite error vector is denoted by $z : \mathbb{R}_{\geq 0} \to \mathbb{R}^{2n}$ representing the concatenation of e and r, all of which are defined as

$$e \triangleq q_d - q, \tag{6}$$

$$r \triangleq \dot{e} + \alpha e, \tag{7}$$

$$z \triangleq \left[e^\top,\ r^\top\right]^\top. \tag{8}$$

The system objective is for the rider with stimulation to track the desired trajectory, while the motor attached to the bike compensates to track the admittance trajectory which is added to offset the desired cadence through the interaction torque. The adjusted admittance error is denoted $\xi : \mathbb{R}_{\geq 0} \to \mathbb{R}^n$, while the filtered tracking error based on ξ is denoted as $\psi : \mathbb{R}_{\geq 0} \to \mathbb{R}^n$. The composite admittance adjusted error vector is the concatenation of ξ and ψ, and is denoted as $\zeta : \mathbb{R}_{\geq 0} \to \mathbb{R}^{2n}$. These adjusted tracking errors are defined as;

$$\xi \triangleq q_a + q_d - q, \tag{9}$$

$$\psi \triangleq \dot{\xi} + \beta\xi, \tag{10}$$

$$\zeta \triangleq \left[\xi^\top,\ \psi^\top\right]^\top, \tag{11}$$

where $q_a : \mathbb{R}_{\geq 0} \to \mathcal{Q}^n$ and $\dot{q}_a,\ \ddot{q}_a : \mathbb{R}_{\geq 0} \to \mathbb{R}^n$ denote the online-generated admitted position, velocity, and acceleration, respectively, and $\beta \in \mathbb{R}_{>0}$ denotes a selectable constant control gain. The admittance trajectory is generated online through the use of an admittance filter designed as

$$e_\tau = M_d\ddot{q}_a + B_d\dot{q}_a + K_d q_a, \tag{12}$$

where $M_d,\ B_d,\ K_d \in \mathbb{R}_{>0}$ are selectable constant positive definite filter constants, shown in the subsequent stability analysis to be passive, and thus energy dissipative [27, Lemma 6.4], which ensures that the admittance trajectory[4] remains bounded. In (12), the interaction torque error between the cycle and its rider is denoted by $e_\tau : \mathbb{R}_{\geq 0} \to \mathbb{R}^n$ and defined $e_\tau \triangleq \tau_{int} - \tau_d$, where $\tau_d : \mathbb{R}_{\geq 0} \to \mathbb{R}^n$ denotes the bounded

[3]For notational brevity, all functional dependencies are hereafter suppressed unless required for clarity of exposition.

[4]For simplicity, the saturated admittance trajectory is henceforth referred to as the admittance trajectory.

desired interaction torque[5], and $\tau_{int} : \mathbb{R}_{\geq 0} \to \mathbb{R}^n$ denotes the bounded measurable interaction torque (i.e., $\|\tau_{int}\|_\infty \in \mathcal{L}_\infty$) [33], [34].

Assumption 1. The measurable interaction torque can be bounded by $\|\tau_{int}\|_\infty \leq c_\tau$, where $c_\tau \in \mathbb{R}_{>0}$ is a unknown constant [33], [34].

The admittance trajectory plays the role of acclimating to the rehabilitation task, providing challenge to the muscles of the rider, and the additional robust and adaptive controllers stabilize the combined system and ensure that the cadence of the whole cycle remain within allowable ranges. The rider is tasked with minimizing the absolute error in (6) and (7), and the difference in the rider's ability to apply force and the tracking error in (6) and (7) is absorbed by the admittance filter. In most experiments, the rider was incapable of providing the necessary torque to track the desired trajectory, due mainly to the saturation of the applied stimulation to account for the comfort of the rider. The robust and adaptive aspects of the controller instead track the admitted error and converge to the admitted trajectory generated by the designed admittance filter.

B. Adaptive Admittance Controller

The main error system with added admittance that is tracked by electric motor actuation, the open-loop system is introduced through (6)-(10), and its relationships to the dynamics is derived from (1) by taking the time derivative of the admittance augmented error ψ, premultiplying by the mass matrix M, and the adding and subtracting the Coriolis matrix through $C\psi$. This results in

$$M\dot{\psi} \quad = \quad T_1 + T_2 - \tau_e - \tau_h + d - C\psi, \tag{13}$$

where $T_1 \triangleq M\ddot{q}_d + C\dot{q} + P + b\dot{q} + G$ and $T_2 \triangleq M\left(\ddot{q}_a + \beta\dot{\xi}\right) + C\psi$. T_1 is composed of terms which are shared between the position and admittance augmented error systems, while T_2 allows for the pseudo-adaptation paradigm by being composed of only admittance terms.

Remark 1. T_1 and T_2 are treated as individual functions, implying a linear separability of these dynamics. Each network is then written in terms of a different subsystem, one compensating for the shared dynamics of both error systems, the other adapting to only the admittance error. Thus, the potentially destabilizing effects of the shared function approximation are both reduced as the complexity of the approximated function is reduced, and the potentially destabilizing effects are compensated for by the function approximation of the other.

The functions $f_{d,1}$ and $f_{d,2}$ are respectively defined as $f_{d,1} \triangleq M\left(q_d + q_a\right)\ddot{q}_d + C\left(q_d + q_a, \dot{q}_d + \dot{q}_a\right)\left(\dot{q}_d + \dot{q}_a\right) + P\left(q_d + q_a, \dot{q}_d + \dot{q}_a\right) + b \cdot \left(\dot{q}_d + \dot{q}_a\right) + G\left(q_d + q_a\right)$, and $f_{d,2} \triangleq M\left(q_d + q_a\right)\ddot{q}_a$. The first function $f_{d,1}$ is constructed explicitly to compensate for the dynamics appearing as a consequence of both r and ψ, while $f_{d,2}$ is designed to compensate for terms that appear only as a consequence of ψ. The terms are added and subtracted to the previous open-loop admittance error system in (13) which can then be rewritten to prepare for the injection of the neural network function approximation

$$M\dot{\psi} = S_1 + S_2 + f_{d,1} + f_{d,2} - \tau_e - \tau_h + d - C\psi, \tag{14}$$

where S_1 and S_2 are functions which can be bounded by Properties 1 and 3 and the Mean Value Theorem as $\|S_j\| \leq c_{j,1}\|\zeta\| + c_{j,2}\|\zeta\|^2$, where $c_{j,i} \in \mathbb{R}_{>0},\ \forall i \in \{1,2\},\ \forall j \in \mathcal{J} \triangleq \{1,2\}$ are known constants, and ζ comes from (11).

Because (12) is passive, Assumption 1 implies $q_a,\ \dot{q}_a,\ \ddot{q}_a$ are restricted to compact sets, and the subsequent stability analysis shows that the trajectory is bounded. Then, let the input vectors composed of the closed sets of the desired and admitted trajectories into each neural network be confined to the compact sets $\mathbb{S}_1 \in \mathbb{R}^{3n+1}$ and $\mathbb{S}_2 \in \mathbb{R}^{4n+1}$. The functions defined by $f_{d,j},\ \forall j \in \mathcal{J}$ according to [35], [36] can be approximated by neural networks composed of the sets of ideal weights and biases, as long as the maps $f_{d,j} : \mathbb{S}_j \to \mathbb{R}^n,\ \forall j \in \mathcal{J}$ where $f_{d,j}$ is continuous are valid. Moreover, by predicating the networks on closed sets (i.e., the desired and admittance trajectories), as opposed to open sets (i.e., the measured trajectory), the subsequent stability analysis is globally valid.

$$f_{d,j} = W_j^\top \rho\left(V_j^\top X_{d,j}\right) + \epsilon_j\left(X_{d,j}\right),\forall j \in \mathcal{J}, \tag{15}$$

where $X_{d,1} \triangleq \begin{bmatrix} 1, & \left(q_d + q_a\right)^\top, & \left(\dot{q}_d + \dot{q}_a\right)^\top, & \ddot{q}_d^\top \end{bmatrix}^\top \in \mathbb{S}_1$ is the ideal bounded input to the first neural network, $V_1 \in \mathbb{R}^{(3n+1)\times L}$, and $W_1 \in \mathbb{R}^{(L+1)\times n}$ are bounded constant ideal weight matrices of the first neural network; $X_{d,2} \triangleq \begin{bmatrix} 1, & \left(q_d + q_a\right)^\top, & \left(\dot{q}_d + \dot{q}_a\right)^\top, & \left(\ddot{q}_a + \beta\dot{q}_a\right)^\top, & \left(\dot{q}_a + \beta q_a\right)^\top \end{bmatrix}^\top \in \mathbb{S}_2$ is the ideal bounded input to the second neural network, and $V_2 \in \mathbb{R}^{(2n+1)\times L}$ and $W_2 \in \mathbb{R}^{(L+1)\times n}$ are bounded constant ideal weight matrices of the second neural network. In addition, the cycling goal reduces the cycle to a cadence tracking objective, and since position is an undbounded value and does not satisfy Property 3, the matrices are altered to $X_{d,1} \triangleq \begin{bmatrix} 1, & 0 \cdot \left(q_d + q_a\right)^\top, & \left(\dot{q}_d + \dot{q}_a\right)^\top, & \ddot{q}_d^\top \end{bmatrix}^\top \in \mathbb{S}_1$, and $X_{d2} \triangleq [\ 1,\ 0 \cdot \left(q_d + q_a\right)^\top,\ \left(\dot{q}_d + \dot{q}_a\right)^\top,\ \left(\ddot{q}_a + \beta\dot{q}_a\right)^\top,\ 0 \cdot \left(\dot{q}_a + \beta q_a\right)^\top]^\top$ implying that the position is represented in the function by only the constant bias. The constant L represents the number of neurons designed in the hidden layer. The function $\rho : \mathbb{R}^L \to \mathbb{R}^{L+1}$ is defined as a vector $\rho \triangleq \begin{bmatrix} 1, & \rho_1, & \rho_2, & ..., & \rho_L \end{bmatrix}^\top$, which applies an element-wise activation function to the vectorial output of $V_j^\top X_{d,j}$, where $\rho_i,\ \forall i \in \{1,\ 2,\ ...,\ L\}$ represents the activation function for each neuron, and the function approximation errors are captured in the bounded value $\epsilon_j : \mathbb{S}_j \to \mathbb{R}^n,\ \forall j \in \mathcal{J}$. The ideal neural network weight matrices V_j and W_j are unknown, thus the estimation for their values in (15), is defined as

$$\hat{f}_{d,j} \triangleq \hat{W}_j^{\ \top} \rho\left(\hat{V}_j^\top X_{d,j}\right), \forall j \in \mathcal{J}, \tag{16}$$

[5]The cycle can be designed to appropriately resist or assist the rider by setting the desired interaction torque to a positive or negative value, respectively.

where $\hat{V}_1 : \mathbb{R}_{\geq 0} \to \mathbb{R}^{(2n+1)\times L}$ and $\hat{W}_1 \in : \mathbb{R}_{\geq 0} \to \mathbb{R}^{(L+1)\times n}$ are the current estimates of V_1 and W_1, respectively, and where $\hat{V}_2 : \mathbb{R}_{\geq 0} \to \mathbb{R}^{(2n+1)\times L}$ and $\hat{W}_2 \in : \mathbb{R}_{\geq 0} \to \mathbb{R}^{(L+1)\times n}$ are the estimates of V_2 and W_2, respectively. Using a Taylor series expansion of the inner layer of the neural network $\rho\left(V_j^\top X_{d,j}\right)$, the approximation $\rho\left(\hat{V}_j^\top X_{d,j}\right)$ of the ideal inner weights and the estimated inner weights can be written as

$$\rho\left(V_j^\intercal X_{d,j}\right) = \hat{\rho}_j + \hat{\rho}_j' \tilde{V}_j^\top X_{d,j} + \mathcal{O}_j^2, \forall j \in \mathcal{J}, \tag{17}$$

where $\hat{\rho}_j \triangleq \rho\left(\hat{V}_j^\top X_{d,j}\right)$, $\hat{\rho}_j' \triangleq \left.\frac{\partial \rho\left(V_j^\top X_{d,j}\right)}{\partial V_j^\top X_{d,j}}\right|_{\hat{V}_j^\top X_{d,j}}$ denotes the partial derivative of ρ about the inner weight vector, and $\mathcal{O}_j^2$ denotes all of the Taylor series terms higher than first order.

Assumption 2. The ideal weights, biases, function approximation errors of (15), and higher-order terms of (17) are bounded [30] and the ideal matrix weights can be bounded by

$$\begin{aligned} \|V\|_F^2 = \text{tr}\left(V^\top V\right) = \text{vec}\left(V\right)^\top \text{vec}\left(V\right) &\leq V_M, \\ \|W\|_F^2 = \text{tr}\left(W^\top W\right) = \text{vec}\left(W\right)^\top \text{vec}\left(W\right) &\leq W_M, \end{aligned}$$

where $\|\cdot\|_F$ is the Frobenius norm of a matrix, tr$(\cdot)$ is the matrix trace rider, the vec(A) rider stacks the columns of a matrix $A \in \mathbb{R}^{m\times n}$ to form a vector vec$(A) \in \mathbb{R}^{mn}$, and $V_M \in \mathbb{R}_{\geq 0}$ and $W_M \in \mathbb{R}_{\geq 0}$ are known positive constants.

From (14) and the to be elucidated stability analysis, the motor controller based on the admittance error is defined as

$$u_e \triangleq B_e^{-1}\left(\hat{f}_{d,1} + \hat{f}_{d,2} + k_1\psi + \xi + \nu\right), \tag{18}$$

where $k_1 \in \mathbb{R}_{>0}$ implements a proportional gain on the filtered tracking error , $\hat{f}_{d,j}$ are defined in (16), and the auxiliary term $\nu : \mathbb{R}_{\geq 0} \to \mathbb{R}^n$ is used to implement a sliding-mode control term defined as $\nu \triangleq \text{sgn}\left(\psi\right)\left(k_2 + k_3\left\|\zeta\right\|^2 + k_4\sigma_h\left\|z\right\|\right)$, where $k_2, k_3, k_4 \in \mathbb{R}_{>0}$ denote constant selectable control gains composing the polynomial state dependent sliding mode error system, sgn$(\cdot)$ denotes the signum function, and z was defined in (8). Substituting (6)-(10) into (14), adding and subtracting $W_j^\top \hat{\rho}_j + \hat{W}_j^\top \hat{\rho}_j' \tilde{V}_j^\top X_{d,j}$, utilizing (17), and inserting the function approximation defined by the Taylor series in (17) fully defines the closed-loop admittance error system as

$$\begin{aligned} M\dot{\psi} = &-\xi - C\psi - k_1\psi - \nu - \tau_h + d \\ &+\tilde{W}_1^\top \hat{\rho}_1 + \hat{W}_1^\top \hat{\rho}_1' \tilde{V}_1^\top X_{d,1} + N_1 + S_1 \\ &+\tilde{W}_2^\top \hat{\rho}_2 + \hat{W}_2^\top \hat{\rho}_2' \tilde{V}_2^\top X_{d,2} + N_2 + S_2, \end{aligned} \tag{19}$$

where the auxiliary functions, which group neural network terms with a finite upper bound $N_1 : \mathbb{R}^{3n+1} \to \mathbb{R}^n$ and $N_2 : \mathbb{R}^{2n+1} \to \mathbb{R}^n$ are defined as

$$N_j \triangleq \tilde{W}_j^\top \hat{\rho}_j' \tilde{V}_j^\top X_{d,j} + W_j^\top \mathcal{O}_j^2 + \epsilon_j, \forall j \in \mathcal{J}, \tag{20}$$

where N_j is bounded by Assumption 2 as $\|N_j\| \leq c_{j,3} \in \mathbb{R}_{>0}$ where $c_{j,3}, \ \forall j \in \mathcal{J}$ are known constants.

Based on the results of the stability analyses for both controllers, the adaptation derivative for each neural network in (16) is generated by the input vectors $X_{d,1}, X_{d,2}$

$$\dot{\hat{W}}_1 = \text{proj}\left(\Gamma_1 \hat{\rho}_1 \psi^\intercal\right), \tag{21}$$

$$\dot{\hat{V}}_1 = \text{proj}\left(\Gamma_2 X_{d,1} \psi^T \hat{W}^\intercal \hat{\rho}_1'\right), \tag{22}$$

$$\dot{\hat{W}}_2 = \text{proj}\left(\Gamma_3 \hat{\rho}_2 \psi^\intercal\right), \tag{23}$$

$$\dot{\hat{V}}_2 = \text{proj}\left(\Gamma_4 X_{d,2} \psi^T \hat{W}_2^\intercal \hat{\rho}_2'\right), \tag{24}$$

with learning gains $\Gamma_i, \forall i = 1, ..4$ where $\Gamma_1 \in \mathbb{R}^{(L+1)\times(L+1)}$, $\Gamma_2 \in \mathbb{R}^{(3n+1)\times(3n+1)}$, $\Gamma_3 \in \mathbb{R}^{(L+1)\times(L+1)}$, $\Gamma_4 \in \mathbb{R}^{(4n+1)\times(4n+1)}$ denote constant positive-definite learning gains, and proj$(\cdot)$ denotes a projection algorithm [37, Section 4.4].

C. Robust Muscle Controller

Admittance control presents an ideal form or dual objective design and human robotic coupling. The rehabilitation task, FES cycling, can be defined in terms of the desired cadence trajectory. However, forcing a human to exactly follow a cadence using unknown force, mechanics, and delay input that is the nature of FES contractions subjects the rider to rapidly changing error direction switching and potentially destabilizing forces. The desired trajectory and desired trajectory error (6) are implemented in the controller through the filtered tracking error (7). The controller for FES is designed to track the desired cadence error using high gain feedback, with the full expectation that the rider's dynamics and contractions may not be capable due to the unknown parameters and saturation of stimulation. The two controllers are coupled, allowing adaptation to be applied to the rider indirectly, termed pseudo-adaptation.

The dynamics are introduced by premultiplying the error vector r by the mass matrix M and substituting the lumped dynamics of (1), reintroducing (6), and (7) to render

$$M\dot{r} = T_1 + T_3 - \tau_e - \tau_h + d - Cr, \tag{25}$$

where T_1 was defined in (13), and $T_3 \triangleq M\alpha\dot{e} + Cr$. Injecting the motor controller (18) and performing some algebraic manipulation then allows (25) to be rewritten as

$$\begin{aligned} M\dot{r} = &-\xi - Cr - k_1\psi - \nu - \tau_h - \hat{f}_{d,2} \\ &+\tilde{f}_{d,1} + T_3 + S_1 + N_1 + d, \end{aligned} \tag{26}$$

where S_1 is defined in (14), ν is defined in (18), N_1 was defined in (20), and $\tilde{f}_{d,1}$ denotes the mismatched weight of the first neural network, defined as $\tilde{f}_{d,1} \triangleq \tilde{W}_1^\top \hat{\rho}_1 + \hat{W}_1^\top \hat{\rho}_1' \tilde{V}_1^\top X_{d,1}$.

Remark 2. Separating the neural networks benefits the tracking objective in two ways. Differing adaptation objectives allow one neural network to adapt to a specific set of dynamics, and the different learning rates additionally offset the errors of each, such that the smaller learning rate should compensate for the errors of the larger. The estimation errors (i.e., $\tilde{W}_j$ and $\tilde{V}_j$) are generated in (26) as N_1 and N_2. The second neural

network estimate appears in (26) in full because it is entirely designed to compensate for terms unique to the admittance error system, and not for terms that appear in the position error system.

Based on (26) and the subsequent stability analysis, the continuous position controller is designed as

$$u_h = B_{\underline{h}}^{-1}(k_5 r), \tag{27}$$

where $k_5 \in \mathbb{R}_{>0}$ denotes a selectable constant muscle control gain, and the lower bound on the muscle control matrix $B_{\underline{h}}$ is introduced in Property 4. Substituting (27) into (26) derives the closed-loop position error system as

$$\begin{aligned} M\dot{r} &= -\xi - Cr - k_1\psi - \nu - B_{\underline{h}}^{-1}(k_5 r) \\ &\quad -\hat{f}_{d,2} + \tilde{f}_{d,1} + T_3 + S_1 + N_1 + d. \end{aligned} \tag{28}$$

Remark 3. As elucidated in the subsequent stability analysis, the muscle controller in (27) is not explicitly required to stabilize the hybrid cycle. The exoskeleton's motors are entirely capable of tracking the admittance trajectory – and because the error systems are coupled (i.e., $\xi = q_a + e$) – stabilizing both error systems simultaneously. For this reason, there is significant freedom in designing the muscle controller and stimulating the rider's muscles for rehabilitative purposes.

IV. Stability Analysis

The designed system constitutes a rehabilitative task and as the contribution of the rider's muscles is difficult to control, the admittance filter allows the interaction between the mechanical and human subsystems at the cost of being unable to drive both errors simultaneously to null. With this design constraint in mind, the stability analyses given instead prove that the admitted controller is Globally Exponentially Stable (GES) i.s.L, and that the absolute cadence error storage function is output feedback passive with respect to the designed controller. Theorem (1) grants exponential convergence using a Lyapunov switched systems analysis directed at the admitted trajectory error in (19). Theorem (2), using a switched systems analysis, proves that the admittance error is output feedback passive with respect to the cadence error in (28) , or in other words, that the deviation from the desired trajectory is bounded with respect to the applied torque of the rider. Theorem (3) combines Theorem (1) and Theorem (2), proving that the admittance error converges while the cadence error remains passive. To facilitate the following analysis, let $V_1 : \mathbb{R}^G \to \mathbb{R}$, where $G = 2n+(n+1)\times L_1+7+1\times L_1+(n+1)\times L_2+10\times L_2$ denote a positive-definite candidate Lyapunov function defined as

$$\begin{aligned} V_{L1}(\eta, t) &\triangleq \frac{1}{2}\psi^\top M\psi + \frac{1}{2}\xi^\top\xi + \frac{1}{2}\text{tr}\left(\tilde{W}_1^\top\Gamma_1^{-1}\tilde{W}_1\right) \\ &\quad + \frac{1}{2}\text{tr}\left(\tilde{V}_1^\top\Gamma_2^{-1}\tilde{V}_1\right) + \frac{1}{2}\text{tr}\left(\tilde{W}_2^\top\Gamma_3^{-1}\tilde{W}_2\right) \\ &\quad + \frac{1}{2}\text{tr}\left(\tilde{V}_2^\top\Gamma_4^{-1}\tilde{V}_2\right), \end{aligned} \tag{29}$$

where $\text{tr}(\cdot)$ is the trace of a matrix, and $\eta : \mathbb{R}_{\geq t_0} \to \mathbb{R}^G$ denotes a composite vector of the states of the admittance error system, defined as $\eta \triangleq \left[\ \xi^\top,\ \psi^\top,\ \text{vec}\left(\tilde{W}_1^\top\right),\ \text{vec}\left(\tilde{V}_1^\top\right),\ \text{vec}\left(\tilde{W}_2^\top\right),\ \text{vec}\left(\tilde{V}_2^\top\right)\ \right]$. It then follows from Property 1 and Assumption 2 that $V_1(\eta)$ can be bounded as $\upsilon_1\|\zeta\|^2 \leq V_1(\eta) \leq \upsilon_2\|\zeta\|^2 + \chi$, where $\upsilon_1,\ \upsilon_2,\ \chi \in \mathbb{R}_{>0}$ are known bounding constants. Additionally, let $V_{L2} : \mathbb{R}^{2n} \to \mathbb{R}$ denote a continuously differentiable, positive-definite storage function defined as

$$V_{L2}(z, t) \triangleq \frac{1}{2}r^\top Mr + \frac{1}{2}e^\top e. \tag{30}$$

Theorem 1. *Given the closed-loop admittance error system in (19), the admittance error system demonstrates global exponential stability in the sense that*

$$\|\zeta(t)\| \leq \kappa_1 \exp(-\kappa_2 t), \tag{31}$$

where $\kappa_1 = V_1(t_0),\ \kappa_2 = \lambda_1 \in \mathbb{R}_{>0}$ are known constants , provided the gains are selected according to the sufficient conditions: $\min\{\beta, k_1\} \geq 3\cdot c_1$, $k_2 \geq c_2$, $k_3 \geq B_{\overline{h}}\cdot B_{\underline{h}}^{-1}(k_4+1)$, where $c_1, c_2 \in \mathbb{R}_{>0}$ are known constants defined as $c_1 \triangleq c_{1,1} + c_{2,1}$ and $c_2 \triangleq c_{1,2} + c_{2,2}$, where $c_{1,1},\ c_{2,1},\ c_{1,2},\ c_{2,2}$ were defined in (14).

Proof: Because the closed-loop error systems in (19) and (21)-(24) are discontinuous, they do not admit classical solutions, and the following analysis will focus on the generalized solutions of (19) and (21)-(24). Using [38] as a framework, let the Filippov regularization of a closed-loop error system be denoted by $K[\cdot]$ and the solutions of the corresponding differential inclusions (i.e., after regularization) be referred to as generalized solutions. Since (32) is continuously differentiable with respect to the states, the Clarke gradient [39] (denoted by ∂V_{L1}) reduces to the standard gradient, i.e., $\partial V_{L1}(\eta, t) = \left\{\left[\ \dot{\zeta}\quad M\psi\quad \tilde{W}_1\Gamma_1^{-1}\quad vec\left(\tilde{V}_1\Gamma_2^{-1}\right)\quad \tilde{W}_2\Gamma_3^{-1}\quad vec\left(\tilde{V}_2\Gamma_4^{-1}\right)\right.\right.$ (1/2) M
Using the calculus of $K[\cdot]$ from [40], a bound on the regularization of the closed-loop error systems in 19 and 21-24 can be computed as $G(\eta, t) \subseteq K[G(\eta, t)]$, where $G : 2n+(n+1)\times L_1+7+1\times L_1+(n+1)\times L_2+10\times L_2$ is defined as $G(\eta, t)\left[\ \dot{\zeta}\quad \dot{\psi}\quad \dot{\tilde{W}}_1^\top\quad \dot{\tilde{V}}_1^\top\quad \dot{\tilde{W}}_2^\top\quad \dot{\tilde{V}}_2^\top\quad 1\ \right]^\top$. Using [38], a bound on the generalized time derivative of the candidate Lyapunov function in 29, $\dot{\tilde{V}}_{L1}$, can be computed as

$$\dot{\tilde{V}}_{L1}(\eta, t) \leq \max_{p\in\partial V_{L1}(\eta,t)} \max_{k\in K[G(\eta,t)]} p^\top h. \tag{32}$$

After substituting (11) and (19) and the update laws (21)-(24), using Property 2, and canceling, (29) can be upper bounded as

$$\dot{\tilde{V}}_{L1} \overset{\text{a.e.}}{=} -\beta\xi^\top\xi - k_1\psi^\top\psi + \psi^\top(S_3 + N_3 - \nu - \tau_h), \tag{33}$$

where ν was defined in (18), $S_3 \triangleq S_1 + S_2$, and $N_3 \triangleq N_1 + N_2 + d$. After substituting (3), (6)-(10), and (27), employing Young's inequality, using Properties 1 and 4, applying the gain

conditions listed in Theorem 1, and upper bounding the result using Properties 1 and 3, (33) can be transformed to

$$\begin{aligned}\dot{\tilde{V}}_1 \overset{\text{a.e.}}{\leq} & -\beta\xi^\top\xi - k_1\psi^\top\psi \\ & - \left|\psi^\top\right|(k_2 - c_3) - \left|\psi^\top\right|(k_3 - c_1)\,||\phi|| \\ & - \left|\psi^\top\right|(k_4 - c_2)\,\|\phi\|^2 - \left|\psi^\top\right|\left(k_5 - B_{\overline{h}}\right)\sigma_h\,|u_h|\,,\end{aligned} \tag{34}$$

where $c_i\ \forall i \in \{1, 2, ..., 5\}$ were defined in Theorem 1. Applying the gain conditions listed in Theorem 1 allows (34) to be upper bounded as

$$\dot{\tilde{V}}_{L1} \overset{\text{a.e.}}{\leq} -\beta\xi^\top\xi - k_1\psi^\top\psi. \tag{35}$$

Using the composite vector ζ defined in (11);

$$\dot{\tilde{V}}_{L1} \overset{\text{a.e.}}{\leq} -\lambda_1\,\|\zeta\|^2\,, \tag{36}$$

where $\lambda_1 \triangleq \min\{\beta, k_1\}$. A further upper bound can be developed using (29) as

$$\dot{\tilde{V}}_{L1} \overset{\text{a.e.}}{\leq} -\lambda_1 V_1, \tag{37}$$

where the components of (29) with admittance error are included. The linear differential inequality of 37can then be solved using Gronwell's inequality as

$$V_1(t) \overset{\text{a.e.}}{\leq} V_1(t_0)\exp(-\lambda_1)\,t. \tag{38}$$

Subsequently, (38) can be used in conjunction with (29) to obtain the result in (31) and conclude $\xi,\ \psi \in \mathcal{L}_\infty$. Furthermore, because (12) is subsequently proven passive, $q_a,\ \dot{q}_a,\ \ddot{q}_a \in \mathcal{L}_\infty$, and it can be concluded from $X_{d,1},\ X_{d,2} \in \mathcal{L}_\infty$. By (21)-(24) and $X_{d,1},\ X_{d,2} \in \mathcal{L}_\infty$, it can be shown $\hat{f}_{d,1},\ \hat{f}_{d,2} \in \mathcal{L}_\infty$. Finally, because $\xi,\ \psi,\ q_a,\ \dot{q}_a \in \mathcal{L}_\infty$, it can be concluded that $e,\ r \in \mathcal{L}_\infty$, and that by (18) and (27), both the admittance and position controllers are bounded (i.e., $u_e,\ u_h \in \mathcal{L}_\infty$). ■

Theorem 2. *The closed-loop position error system in (28) is output strictly passive $\forall t$, with $y = r$, and $u = \left|\tilde{f}_{d,1} + \hat{f}_{d,2} + h(\zeta, \phi)\right|$.*

Proof: Similar to Theorem 1, because of the discontinuity in the admittance controller in (18), the time derivative of (30) exists almost everywhere. Using a similar procedure wherein $\partial V_{L2}(z,t) = \left\{\begin{bmatrix} \dot{z} & Mz & (1/2)\,Mz^2 \end{bmatrix}\right\}$, the calculus of $K[\cdot]$,and the function $H(\eta, t) \subseteq K[H(\eta, t)]$, a similar bound can be derived as

$$\dot{\tilde{V}}_{L2}(\eta, t) \leq \max_{p \in \partial V_{L1}(\eta,t)} \max_{k \in K[G(\eta,t)]} p^\top h. \tag{39}$$

After substituting (6), (7), (18), and (28), using Properties 1, 2, and 4, the time derivative of (30) can be expressed as

$$\begin{aligned}\dot{\tilde{V}}_{L2} \overset{\text{a.e.}}{=} & \ e^\top(r - \alpha e) + \\ & + r^\top\Big(-\xi - k_1\psi - \nu - B_h\sigma_h B_{\underline{h}}^{-1}(k_5 r) \\ & - \hat{f}_{d,2} + \tilde{f}_{d,1} + T_3 + S_1 + N_1 + d\Big).\end{aligned} \tag{40}$$

After substituting (9), (10), performing cancellations, using Property 3, (40) can be bounded as

$$\begin{aligned}\dot{\tilde{V}}_{L2} \overset{\text{a.e.}}{\leq} & -\alpha e^\top e - k_5 r^\top r, \\ & + \|r\|\left|\tilde{f}_{d,1} + \hat{f}_{d,2} + h(\zeta, \phi)\right|,\end{aligned} \tag{41}$$

where $h(\zeta, \phi) : \mathbb{R}^{5n} \to \mathbb{R}$ is a known radially unbounded, strictly increasing function defined as $h \triangleq c_1 + c_2\,\|\zeta\| + c_3\,\|\zeta\|^2 + c_4\,\|\phi\| + c_5\,\|\phi\|^2 +$. Using $\lambda_2 = min\{\alpha,\ k_5\}$, this can be rewritten as

$$\dot{\tilde{V}}_{L2} \overset{\text{a.e.}}{\leq} -\lambda_2\,\|z\|^2 + \|z\|\left|\tilde{f}_{d,1} + \hat{f}_{d,2} + h(\zeta, \phi)\right|. \tag{42}$$

This equation an be written as in [27, Definition 6.3], showing that the position error system e and its further designed filtered tracking version r is output feedback passive within the composite error z. The form $\dot{V} \overset{\text{a.e.}}{\leq} -y\rho(y) + u^\top y$ is analogous to $\dot{V}_{L2}$ where $u^\top \triangleq \left|\tilde{f}_{d,1} + \hat{f}_{d,2} + h(\zeta, \phi)\right|$, the output vector $y = \|z\|$ and $\rho(y) \triangleq \lambda_2\,\|z\| > 0,\ \forall z \neq 0$. The idea of shared learning comes from the fact that the difference between the position and admittance systems $||r^\top - \psi^\top||$ is motivated by the aproximation error of the first neural network, $\epsilon(X_{d,1})$ that comes from the mismatched weights $\tilde{W}$and $\tilde{V}$ and the system disturbance d which represents constant bounded terms. The filtered overall tracking error $||r^\top||$ is a result of the addition of the second neural network $\hat{f}_{d,2}$ and the admittance errors ζ, ϕ, with convergence in the limit for $\zeta,\ \phi$. ■

Theorem 3. *Given the closed-loop admittance error system in (19), and the closed-loop position error system in (28), the combined composite error system $\Omega \triangleq \left[\zeta^\top\ z^\top\right]^\top$ is output strictly passive provided the sufficient gain conditions in Theorems 1 and 2 are satisfied.*

Proof: Considering $V_1(\eta_1)$ in (29) as a candidate Lyapunov function, it can be combined with $V_2(\eta_2)$ in (30) to form a total tertiary storage function $V_3(\eta_1, \eta_2) \triangleq V_1(\eta_1) + V_2(\eta_2)$ for the combined system. The derivatives $\dot{V}_1$ and $\dot{V}_2$ in (35) and (41) can then be summed to yield

$$\dot{V}_{L3} = -\lambda_1\,\|\zeta\|^2 - \lambda_2\,\|z\|^2 + \|z\|\left|\tilde{f}_{d,1} + \hat{f}_{d,2} + h(\zeta, \phi)\right|,$$

allowing for the composite vector $\Omega = [\zeta^\top\ z^\top\ \phi^\top]$ to be utilized, the candidate function derivative can be upper bounded;

$$\dot{V}_{L3} \overset{\text{a.e.}}{\leq} -\min(\lambda_1,\ \lambda_2)\,\|\Omega\|^2 + \max(c_1,\ u_1,\ u_2)\,\|\Omega\|\,,$$

where $c_1,\ \lambda_1$ were defined in (35), and λ_2, u_1, u_2 were defined in (41). Hence, [27, Definition 6.3] can be invoked to show the combined system is *strictly* output passive with the bounded input $u_3 \triangleq \max(c_1,\ u_1,\ u_2)$, output $y_3 \triangleq \|\Omega\|$, and storage function $V_3(\eta_1, \eta_2)$. Simultaneously, the results from Theorems 1 and 2 still hold, which can be used to conclude that while the combined error system remains passive, the admittance error from V_1 still demonstrates globally exponential convergence to a uniform ultimate bound. ■

V. EXPERIMENTS

A. Experimental Materials

The FES cycle used in this work was a lower body reclining tricycle (TerraTrike Rover), modified to provide sensing and actuation. To couple the rider to the bike, orthotic boots (Ossur Rebound Air Tall) were attached to the pedals to preserve alignment with the pedals, and the stimulation was applied using a USB-connected stimulator (Hasomed Rehastim) through self-adhesive electrodes (PALS) attached to the rider's quadriceps, hamstrings, and gluteal muscles, at 70 mA and 60 Hz. The pulse width is adjusted based on feedback and rider comfort. The 24-V, 250-W motor (Unite Motor Company Ltd., MY1016Z2) was attached to the drivetrain of the bike and powered according to (9), through an ADVANCED Motion Controls (AMC) PS300W24 power supply and AMC AB25A100 motor driver, to assist in pedaling. The bike is held stationary and the rear wheel is allowed to rotate freely. A filter card (AMC FC15030) attached in line to the motor reduces noise. This configuration reduces to a single degree of freedom system where the pedal crank angle represents the joint in question. Finally, the desktop housing the MATLAB/Simulink/Quarc program interfaces with the configuration through a Quanser Q-PIDe data acquisition board sampled at 500 Hz. An experimental subject attached to the reclining tricycle is depicted in Figure 1.

As the cycle dynamics are continuous and the crank trajectory does not exist in a finite set, the saturated admitted joint angles were removed and the admittance filter was tied directly to the cadence tracking objective. Since the rehabilitative task was cadence dependent, the position gain of the admittance filter was held as null.

The various gains and initializations set for the controller can be described as follows. The motor gains k_1, k_2, k_3, k_4 were set as $2.5, 0.1, 0.01, 0.01$, respectively. The position gains were set as $\alpha = 1.5$ and $\beta = 1.0$. The muscle gain k_5 was set as 4. The neural networks $\hat{f}_1$ and $\hat{f}_2$ has the following matrix initializations of $\hat{W}_1, \hat{W}_2 \in \mathbb{R}^{1\times 5} = [0, 0, 0, 0, 0]$, with a saturation of ± 0.05 on the individual nodes. For the inner weight networks, $\hat{V}_1 \in \mathbb{R}^{5\times 4}$ and $\hat{V}_2 \in \mathbb{R}^{5\times 5}$, the initializations are set such that there are no redundant weights in each individual network;

$$\hat{V}_{1,init} = \begin{bmatrix} 0.18 & 0.19 & 0.2 & 0.21 & 0.22 \\ 0.58 & 0.59 & 0.6 & 0.61 & 0.62 \\ 0.08 & 0.09 & 0.1 & 0.11 & 0.12 \\ 0.67 & 0.35 & 0.33 & 0.19 & 0.18 \end{bmatrix} \cdot 0.1$$

$$\hat{V}_{2,init} = \begin{bmatrix} 0.18 & 0.19 & 0.2 & 0.21 & 0.22 \\ 0.58 & 0.59 & 0.6 & 0.61 & 0.62 \\ 0.08 & 0.09 & 0.1 & 0.11 & 0.12 \\ 0.67 & 0.35 & 0.33 & 0.19 & 0.18 \\ 0.45 & 0.76 & 0.8 & 0.54 & 0.17 \end{bmatrix} \cdot 0.01$$

with a saturation of ± 8 on the individual nodes. The learning gains, which correspond to $\hat{W}_1, \hat{V}_1, \hat{W}_2, \hat{V}_2$, respectively, were selected as $\Gamma_1 = \text{diag}([0.11,\ 0.06,\ 0.08,\ 0.09,\ 0.1,\ 0.07] \cdot 0.006)$, $\Gamma_2 = \text{diag}([0.8\ \ 0.2\ \ 2.0\ \ 4.0] \cdot 6)$ $\Gamma_3 = \text{diag}([0.11,\ \ 0.06,\ 0.08,\ 0.09,\ ,0.1\ ,0.07] \cdot 0.012)$, $\Gamma_4 = \text{diag}([0.8,\ 0.2,\ 2.0,\ 4.0] \cdot 1.2)$, where $\text{diag}(\cdot)$ indicates the operation transforming the vector into a diagonal matrix. the final values of each individual neuron is determined by the random adaptation to the specific subject, but the overall contribution of the neural network feedforward terms is given in Table II. Redundancy in the selection of the initializations is offset by the differing learning rates.

B. Experimental Methods

For comparison, two types of controllers were run, an adaptive controller including the neural network elements, and a robust controller where neural network contribution was turned off. The experimental protocols include 8 subjects with 8 separate cycling events, including both stimulated and unstimulated protocols. These were separated over the course of at least two days to avoid the effects of fatigue from repeated stimulation, 4 events on one day, and 4 on a separate day. The experimental procedures were chosen such that stimulated and unstimulated events alternated so that 2 stimulated events occurred per day and two unstimulated. For stimulated protocols, the total experiment duration was 180 sec, including ramp-up to steady state at 30 sec where no stimulation or adaptation occurred. Unstimulated events lasted for 300 sec including the previously mentioned ramp-up period and each included two experimental protocols, one where learning adaptation occurred with no external disturbance, up until 180 sec, and from 180 sec to 300 sec learning adaptation was turned off with the neural network fixed, and a Gausian distributed disturbance was added to the motor current command with mean 0.000, standard deviation 0.175. In summary, for each subject, there are twelve sets of statistics drawn from the set of experiments based on 4 protocols, adaptive or merely robust, a cadence of 30 or 50 RPM, and stimulated or unstimulated. For the unstimulated case, the experiments have an additional 120 sec with added noise and learning adaptation turned off.

To promote subject comfort, muscular stimulation is saturated on the bike. The experimental setup step includes a ramp up period where the subject is slowly acclimated to the motion of the cycle, and then at steady cadence by acclimating the subject to stimulation until the tacking objective is achieved or the measured saturation limit is achieved. This value is measured by beginning a normal cycling task on the bike with very low stimulation, on the order of 20 ms, and then slowly increasing the stimulation value by 5 ms until the subject reports that the value is tolerable, to ensure a sufficient muscular contraction. For most subjects, the stimulation threshold was insufficient to ensure that the desired trajectory was tracked, but sufficient to fulfill the stimulation objective. The maximum stimulation achieved by any single subject was 80 ms, while the minimum was 30 ms. Of note, while the subject was

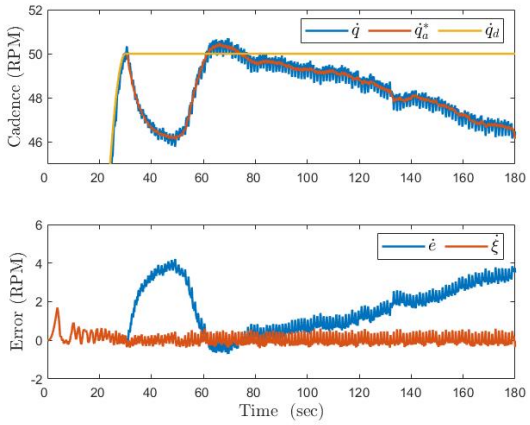

Fig. 2. Example tracking results of the stimulated robust protocol at 50 RPM. The early onset of fatigue can be seen as well as notable experiment features such as convergence to the desired trajectory as stimulation increases, the end of the 30 sec ramp up period, and the difference between the desired and admitted trajectories.

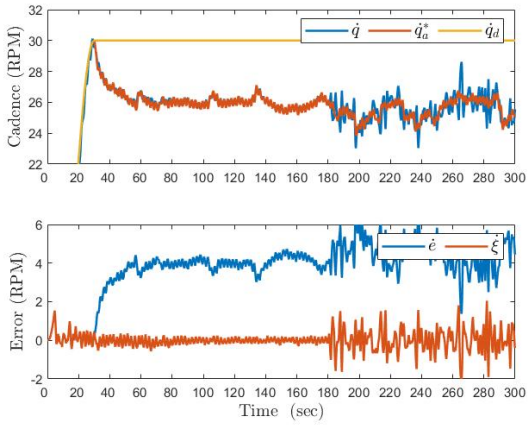

Fig. 3. Example tracking results of the unstimulated adaptive protocol at 30 RPM. This experiment includes two cases, one where the unstimulated rider allows passive cycling, and one where noise is added to the motor input at $t = 180\ sec.$

saturated at 80 ms, the limit was not achieved during cycling as the muscle controller was able to achieve adequate input to drive the admitted trajectory to the desired.

In addition to the eight subjects that had no spinal injury, an additional subject with a spinal injury, who shall be referred to as subject 9, was subjected to an alternative protocol to quantify the rehabilitation task. The statistics for this subject are given in Table IV. Finally, for the subject with a neurological condition, there were a total of three protocols. The first was nonvoluntary cycling with the previously mentioned ramp-up period of 30 sec, then with stimulation and the adaptive controller active, with a total experiment duration of 240 sec. The second protocol was the same ramp-up protocol, duration and nonvolitional protocol. Subject 9 performed two passive protocols, one using the neural network adaptive controller, and the other the robust controller, and one active protocol,

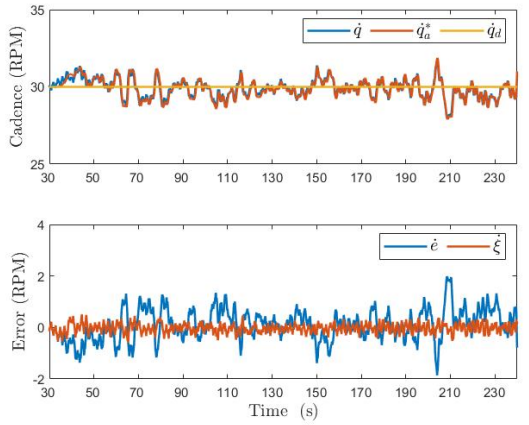

Fig. 4. Tracking for the volitional protocol of Subject 9 beginning after ramp up at $t = 30$ sec. Subject 9 is capable of reasonably tracking the desired trajectory volitionally.

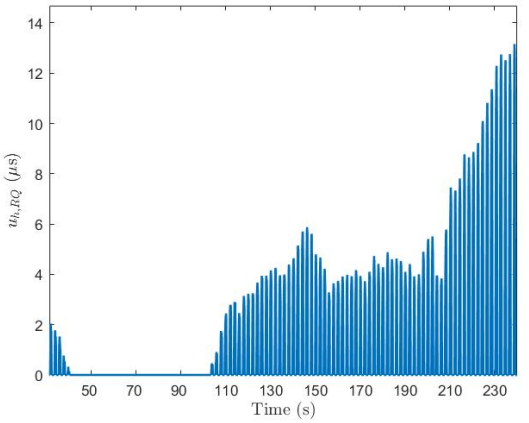

Fig. 5. An example of muscle stimulation for the right quadriceps during the volitional pedaling protocol. The low stimulation parameters correlates to the ability of Subject 9 to track the objective volitionally, though fatigue causes the stimulation to increase roughly linearly at $t \approx 210$ sec.

where the subject was tasked with attempting to voluntarily track the desired trajectory while it appeared on the computer running Simulink.

All experimental procedures were approved by the University of Alabama under IRB Protocol #20-005-ME.

C. Results and Discussion

Table III shows the various subjects, protocols, control efforts, and error results of the experimental procedures. Comparisons are made between the mean absolute average error, and the P-value for the comparisons generated using a Friedman test of the datasets. The P-value represents the likelihood of a type one error on the null hypothesis, that there is a measureable difference between the controller. The margin for statistical signifigance is P=0.05, or a 5 percent chance of the type one error.

TABLE I
PROTOCOL COMPARISONS

Protocol	Mean $\dot{\xi}$(RPM)	Average std. $\dot{\xi}$(RPM)
Adaptive	0.0337	0.796
Robust	0.0179	0.874
Adaptive with Stimulation	0.0402	0.663
Robust with Stimulation	0.0105	0.757
Adaptive with Noise	0.0199	1.0506
Robust with Noise	0.0204	1.174
Adaptive no Addition	0.0409	0.676
Robust no Addition	0.0168	0.692
Adaptive 50 RPM	0.0362	0.855
Robust 50 RPM	0.0190	0.866
Adaptive 30 RPM	0.0312	0.738
Robust 30 RPM	0.0167	0.883

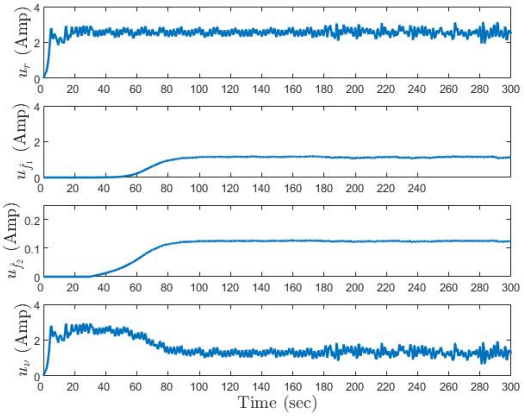

Fig. 6. The contribution of the motor control term u_m. (Top) is the total term, second from top is the neural network $\hat{f}_1$, third from top shows the second neural network contribution $\hat{f}_2$. Bottom is the combination of the proportional filtered tracking gain k_1 and sliding mode terms. The effort of the neural networks increases until plateauing at $t \approx 90$ sec, and the contribution is well divided between feedforward and feedback terms.

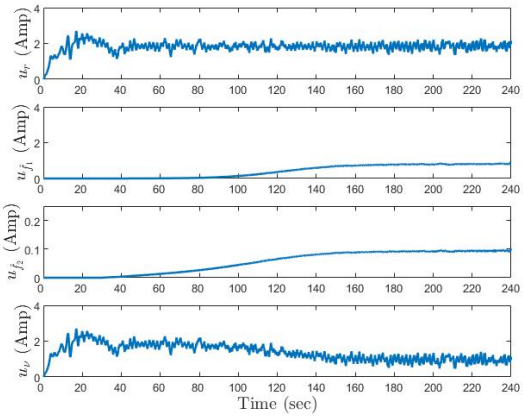

Fig. 7. The contribution to the motor control term u_m as in Fig. 6 for the volitional pedaling protocol for the Subject 9. The effort of the neural networks increases until plateauing at $t \approx 150$ sec, implying that adaptation to dynamics is slower for volitional pedaling. In the future adaptation results can be saved and loaded for particular subjects, instead of beginning each time.

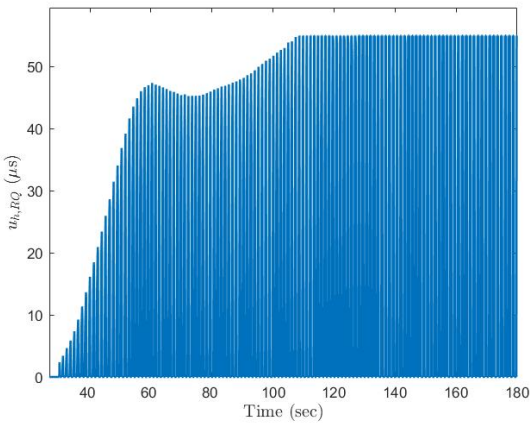

Fig. 8. An example of muscle stimulation for the right quadriceps during an experiment. As the tracking objective is achieved at $t \approx 60$ sec stimulation plateaus or decreases, but as fatigue sets stimulation increases to saturation at $t \approx 110$ sec.

For the overall performance of the two controllers, the average mean error $\dot{\xi}$ for the robust controller was 0.0179 RPM, while the adaptive controller was larger, at 0.0337 RPM, with a P-value of $1.49 \cdot 10^{-5}$. However, the larger standard deviation of error for the adaptive and robust controllers are 0.796 and 0.874 RPM respectively, a 9.0% improvement, with a P-value of 0.02, indicating that both differences are statistically significant. The scale of the standard deviation to mean indicates that the standard deviation is a better indicator of controller performance and a smaller standard deviation is considered smoother i.e. less deviation in error values. The largest difference in standard deviation manifested for the noisy protocol, with a P-value of $2.7 \cdot 10^{-3}$, indicating statistical significance.

The means for these two protocols had a P-value of 0.62, with no statistical significance, thus the largest difference in performance between the two controllers is under noisy conditions, with a 10.5% improvement in average standard deviation over the roust controllers. Other P-values indicating statistical significance are the mean of the adaptive and robust controllers with no additional noise, $6.33 \cdot 10^{-5}$, and the mean of the adaptive and robust controllers with stimulation, $6.33 \cdot 10^{-5}$. Protocols not showing statistical significance are the average standard deviation of the adaptive and robust controllers with stimulation, 0.617.

Lastly, the various protocols under the same controller were tested for statistical significance. The adaptive controller showed much larger statistical significance between protocols, P-value of $3.50 \cdot 10^{-6}$, and the robust controller showed a less but still significantly different P-value of $9.90 \cdot 10^{-3}$. This indicates that differences in performance on each individual controller under the different protocols were a product of the controller itself.

TABLE II
EXAMPLE NEURAL NETWORK MOTOR CONTRIBUTION

Subject	stimulation	$\dot{q}_d$ (RPM)	noise	u_m mean (Amp)	$\hat{f}_1$ mean (Amp)	$\hat{f}_2$ mean (Amp)
2	stimulated	50	none	3.01±0.45	1.20±0.44	0.09±0.03
		30		2.71±0.49	0.92±0.46	0.11±0.04
	unstimulated	50		3.38±0.46	1.33±0.48	0.12±0.04
		30		2.67±0.46	0.87±0.46	0.11±0.05
		50	added	3.41±0.61	1.50±0.04	0.14±0.00
		30		2.64±0.52	1.19±0.02	0.15±0.00
4	stimulated	50	none	2.78±0.72	1.10±0.41	0.08±0.02
		30		2.61±0.50	0.89±0.44	0.10±0.04
	unstimulated	50		3.01±0.84	1.21±0.44	0.08±0.02
		30		2.79±0.44	0.97±0.47	0.10±0.04
		50	added	2.94±0.91	1.41±0.01	0.10±0.00
		30		2.75±0.53	1.25±0.02	0.12±0.00

For the cycling cadence protocols, the means of the two controllers at 50 RPM show a statistical difference, with a P-value of $2.29 \cdot 10^{-4}$. This is also the case but to a lesser extent for the controllers at 30 RPM, with a P-value of $1.43 \cdot 10^{-2}$. The standard deviations are of more interest as previously noted, and the P-value for adaptive vs. robust control does not show statistical significance, 0.68. Finally, the results at 30 RPM do show statistical significance, with a low P-value of $4.33 \cdot 10^{-3}$, indicating that the difference in performance is a result of the inherent controller properties. This is possibly due to the slower speed allowing a better adaptation to the cycle and rider dynamics. To verify this proposition, the performance of the controllers was compared to themselves, adaptive at 30 RPM and 50 RPM and robust at 30 and 50 RPM. The robust controller shows no statistical significance, with the P-value for the mean at 0.22 and the standard deviation of 0.41. The adaptive controller, on the other hand, shows statistical significance in both cases, with a P-value of $4.33 \cdot 10^{-3}$ for the means, and $4.12 \cdot 10^{-2}$ for the standard deviations.

In Table II the offloading of the feedback term to the feedforward adaptive term can be examined. The combined neural network terms represent a significant portion of the control effort. The mean contribution of the Neural network terms is 1.25 Amp, with an average standard deviation of 0.31 Amp for the first neural network, and 0.03 Amp for the second. This composes about 44% of the total control effort, which is evenly divided between feedforward and feedback terms.

Finally, for the neurological participant, the relevant statistics are shown in Table IV. Because there was only one subject in this particular protocol, statistical significance cannot be drawn from the data. The performance of the controllers was similar to previous data and subjects, albeit closer, with only a 5.8% improvement in the standard deviation from adaptive control over robust and half the average error of the robust over the adaptive.

VI. CONCLUSION

Hybrid exoskeletons present a strategy in rehabilitation of people with neurological conditions. To address the rehabilitation objective, a neural network adaptive controller was implemented on a hybrid FES cycling System with closed-loop control, and a robust controller was utilized to stimulate the muscles of the cycle's rider. The cycle is paired to the rider using an admittance filter, guaranteeing safety, and using a Lyapunov-based stability analysis the augmented admittance error is proven globally exponentially stable, while the admittance filter is proven output feedback passive with respect to the cadence error. Eight experimental subjects without neurological conditions were subjected to 12 different experimental protocols combining variance in cadence, noise addition, stimulation, and two types of controllers. The neural network adaptive controller demonstrates a larger mean error, but smaller standard deviation of error than the robust controller. Composite statistics were quantified using a Friedman test of statistical significance for the results. To quantify the rehabilitative task, an additional subject with a neurological condition was recruited and subjected to three protocols, two incorporating a variance in controller and one where pedaling was done volitionally. Future work should aim to measure the results of the FES system over repeated rehabilitation sessions.

REFERENCES

[1] S. E. Wallace and M. L. Kimbarow, *Cognitive Communication Disorders*. Plural Publishing, 2016.

[2] E. J. Benjamin, M. J. Blaha, S. E. Chiuve, M. Cushman, S. R. Das, R. Deo, S. D. de Ferranti, J. Floyd, M. Fornage *et al.*, "Heart disease and stroke statistics - 2017 update," *Circulation*, vol. 135, no. 10, pp. 146–603, 2017.

[3] J. H. Rimmer and J. L. Rowland, "Health promotion for people with disabilities: implications for empowering the person and promoting disability-friendly environments," *Am. J. Lifestyle Med.*, vol. 2, no. 5, pp. 409–420, 2008.

[4] M. Bélanger, R. B. Stein, G. D. Wheeler, T. Gordon, and B. Leduc, "Electrical stimulation: can it increase muscle strength and reverse osteopenia in spinal cord injured individuals?" *Arch. Phys. Med. Rehabil.*, vol. 81, no. 8, pp. 1090–1098, 2000.

[5] S. Ferrante, A. Pedrocchi, G. Ferrigno, and F. Molteni, "Cycling induced by functional electrical stimulation improves the muscular strength and the motor control of individuals with post-acute stroke," *Eur. J. Phys. Rehabil. Med.*, vol. 44, no. 2, pp. 159–167, 2008.

[6] T. Mohr, J. Pødenphant, F. Biering-Sørensen, H. Galbo, G. Thamsborg, and M. Kjær, "Increased bone mineral density after prolonged electrically induced cycle training of paralyzed limbs in spinal cord injured man," *Calcif. Tissue Int.*, vol. 61, no. 1, pp. 22–25, 1997.

TABLE III
EXAMPLE RESULTS OF VARIOUS PROTOCOLS

Subject	Stimulation	Controller	Cadence (RPM)	noise	$\dot{\xi}$ mean(RPM)	$\dot{e}$ mean (RPM)	$\dot{q}_a$ mean (RPM)	u_m mean (Amp)	τ_{int} mean (N·m)
2	stimulated	Adaptive	50	none	-0.05±0.49	4.97±0.91	-5.02±0.78	3.01±0.45	-1.09±0.80
			30		-0.05±0.57	3.01±0.89	-3.06±0.78	2.71±0.49	-0.66±1.52
		Robust	50		-0.01±0.45	5.87±0.95	-5.88±0.86	3.09±0.27	-1.27±0.66
			30		-0.01±0.57	3.92±0.96	-3.93±0.84	2.61±0.34	-0.85±1.14
	unstimulated	Adaptive	50		-0.04±0.47	9.71±1.46	-9.75±1.41	3.38±0.46	-2.12±0.97
			30		-0.03±0.53	5.42±0.95	-5.46±0.85	2.67±0.46	-1.18±1.37
		Robust	50		-0.02±0.56	8.22±1.78	-8.24±1.70	3.25±0.34	-1.77±1.00
			30		-0.01±0.55	4.93±0.79	-4.94±0.65	2.69±0.33	-1.07±1.10
		Adaptive	50	added	-0.03±1.01	12.45±1.44	-12.49±1.05	3.41±0.61	-2.62±1.38
			30		-0.02±0.93	4.84±0.96	-4.86±0.40	2.64±0.52	-1.02±1.07
		Robust	50		-0.02±1.15	7.25±1.47	-7.27±1.00	3.13±0.49	-1.52±0.95
			30		-0.02±1.15	5.37±1.13	-5.39±0.39	2.66±0.51	-1.13±1.16
4	stimulated	Adaptive	50	none	-0.04±0.97	0.88±1.39	-0.92±1.08	2.78±0.72	-0.20±1.53
			30		-0.03±0.61	0.65±1.25	-0.69±1.17	2.61±0.50	-0.15±1.36
		Robust	50		-0.01±1.28	1.65±1.77	-1.67±1.26	2.97±0.76	-0.38±1.57
			30		-0.01±1.11	0.72±1.49	-0.73±1.11	2.48±0.70	-0.15±1.61
	unstimulated	Adaptive	50		-0.04±1.17	3.71±1.27	-3.75±0.56	3.01±0.84	-0.81±1.33
			30		-0.03±0.51	2.84±0.68	-2.87±0.56	2.79±0.44	-0.63±0.86
		Robust	50		-0.01±0.68	4.72±1.01	-4.73±0.77	3.10±0.40	-1.02±1.05
			30		-0.01±0.55	3.10±0.66	-3.11±0.42	2.60±0.33	-0.67±0.77
		Adaptive	50	added	-0.03±1.46	3.85±1.43	-3.88±0.24	2.94±0.91	-0.81±1.32
			30		-0.02±0.99	3.34±1.01	-3.36±0.41	2.75±0.53	-0.70±0.89
		Robust	50		-0.02±1.19	5.47±1.19	-5.49±0.30	3.05±0.52	-1.16±0.92
			30		-0.02±1.13	3.09±1.12	-3.11±0.34	2.56±0.50	-0.64±0.75

TABLE IV
STATISTICS FOR SUBJECT 9

Protocol	$\dot{\xi}$ (RPM)	$\dot{e}$ (RPM)	$\dot{q}_a$ (RPM)	u_m (Amp)	$\hat{f}_1$ mean (Amp)	$\hat{f}_2$ mean (Amp)	τ_{int} mean (N·m)	$\dot{q}$ mean (RPM)
Adaptive	-0.04±0.86	5.32±1.72	-5.36±1.55	2.1±0.8	0.49±0.37	0.08±0.04	1.21±2.33	24.68±1.72
Robust	-0.02±0.81	3.82±1.36	-3.84±1.17	2.03±0.71	NA	NA	1.55±2.17	26.18±1.36
Adaptive Volitional	-0.03±0.73	0.1±0.92	-0.13±0.75	1.83±0.7	0.44±0.34	0.06±0.03	2.52±2.35	29.9±0.92

[7] A. J. del Ama, Á. Gil-Agudo, J. L. Pons, and J. C. Moreno, "Hybrid FES-robot cooperative control of ambulatory gait rehabilitation exoskeleton," *J. Neuroeng. Rehab.*, vol. 11, no. 1, p. 27, 2014.

[8] K. J. Hunt, D. Hosmann, M. Grob, and J. Saengsuwan, "Metabolic efficiency of volitional and electrically stimulated cycling in able-bodied subjects," *Med. Eng. Phys.*, vol. 35, no. 7, pp. 919–925, Jul. 2013.

[9] S. Haddadin, A. Albu-Schaffer, A. De Luca, and G. Hirzinger, "Collision detection and reaction: A contribution to safe physical human-robot interaction," in *Proc. IEEE/RSJ Int. Conf. Intell. Robot. Sys. (IROS)*. IEEE, 2008, pp. 3356–3363.

[10] S. Haddadin, A. Albu-Schäffer, and G. Hirzinger, "Safety analysis for a human-friendly manipulator," *Int. J. Soc. Robot.*, vol. 2, no. 3, pp. 235–252, 2010.

[11] C.-S. Poon, "Sensorimotor learning and information processing by bayesian internal models," in *IEEE Proc. Eng. Med. Biol. Soc.*, vol. 2. IEEE, 2004, pp. 4481–4482.

[12] P. M. Rossini and G. Dal Forno, "Integrated technology for evaluation of brain function and neural plasticity," *Phys. Med. Rehabil. Clin. N. Am.*, vol. 15, no. 1, pp. 263–306, 2004.

[13] J. Stein, H. I. Krebs, W. R. Frontera, S. E. Fasoli, R. Hughes, and N. Hogan, "Comparison of two techniques of robot-aided upper limb exercise training after stroke," *Am. J. Phys. Med. Rehabil.*, vol. 83, no. 9, pp. 720–728, 2004.

[14] A. J. Del-Ama, A. D. Koutsou, J. C. Moreno, A. De-Los-Reyes, Á. Gil-Agudo, and J. L. Pons, "Review of hybrid exoskeletons to restore gait following spinal cord injury," *J. Rehabil. Res. Dev.*, vol. 49, no. 4, pp. 497–514, 2012.

[15] F. Anaya, P. Thangavel, and H. Yu, "Hybrid FES–robotic gait rehabilitation technologies: a review on mechanical design, actuation, and control strategies," *Int. J. Intell. Robot. Appl.*, pp. 1–28, 2018.

[16] N. Hogan, "Impedance control: An approach to manipulation: Parts I, II, III," *J. Dyn. Syst. Meas. Control*, vol. 107, pp. 1–24, 1985.

[17] I. Ranatunga, F. L. Lewis, D. O. Popa, and S. M. Tousif, "Adaptive admittance control for human–robot interaction using model reference design and adaptive inverse filtering," *IEEE Trans. Control Sys. Tech.*, vol. 25, no. 1, pp. 278–285, 2017.

[18] G. Herrnstadt and C. Menon, "Admittance-based voluntary-driven motion with speed-controlled tremor rejection," *IEEE/ASME Trans. Mech.*, vol. 21, no. 4, pp. 2108–2119, 2016.

[19] Q. Wu, X. Wang, B. Chen, and H. Wu, "Development of a minimal-intervention-based admittance control strategy for upper extremity rehabilitation exoskeleton," *IEEE Trans. Syst. Man Cybern: Sys.*, 2017.

[20] C. A. Cousin, C. A. Rouse, V. H. Duenas, and W. E. Dixon, "Controlling the cadence and admittance of a functional electrical stimulation cycle," *IEEE Trans. Neural Syst. Rehabil. Eng.*, vol. 27, no. 6, pp. 1181–1192, June 2019.

[21] C. A. Cousin, P. Deptula, C. Rouse, and W. E. Dixon, "Cycling with functional electrical stimulation and adaptive neural network admittance control," in *Proc. Am. Control Conf.*, 2019, pp. 1742–1747.

[22] V. H. Duenas, C. A. Cousin, V. Ghanbari, and W. E. Dixon, "Passivity-based learning control for torque and cadence tracking in functional electrical stimulation FES induced cycling," in *Proc. Am. Control Conf.*, 2018, pp. 3726–3731.

[23] V. Duenas, C. A. Cousin, C. Rouse, and W. E. Dixon, "Extremum

seeking control for power tracking via functional electrical stimulation," in *Proc. IFAC Conf. Cyber. Phys. Hum. Syst.*, 2018, pp. 164–169.
[24] V. Duenas, C. A. Cousin, V. Ghanbari, E. J. Fox, and W. E. Dixon, "Torque and cadence tracking in functional electrical stimulation induced cycling using passivity-based spatial repetitive learning control," *Automatica*, vol. 115, p. 108852, 2020.
[25] C. A. Cousin, V. Duenas, C. Rouse, M. Bellman, P. Freeborn, E. Fox, and W. E. Dixon, "Closed-loop cadence and instantaneous power control on a motorized functional electrical stimulation cycle," *IEEE Trans. Control Sys. Tech.*, vol. 28, no. 6, pp. 2276–2291, 2020.
[26] C. A. Cousin, C. A. Rouse, and W. E. Dixon, "Split-crank functional electrical stimulation cycling: An adapting admitting rehabilitation robot," *IEEE Trans. Control Syst. Tech.*, vol. 29, no. 5, pp. 2153–2165, 2020.
[27] H. K. Khalil, *Nonlinear Systems*, 3rd ed. Upper Saddle River, NJ: Prentice Hall, 2002.
[28] H. Khalil and F. Esfandiari, "Semiglobal stabilization of a class of nonlinear systems using output feedback," *IEEE Trans. Autom. Control*, vol. 38, no. 9, pp. 1412–1415, 1993.
[29] C. A. Cousin, P. Deptula, C. A. Rouse, and W. E. Dixon, "A switched lyapunov-passivity approach to motorized fes cycling using adaptive admittance control," *IEEE Trans. Control Syst. Tech.*, vol. 30, no. 2, pp. 740–754, 2022.
[30] A. Behal, W. E. Dixon, B. Xian, and D. M. Dawson, *Lyapunov-Based Control of Robotic Systems*. Taylor and Francis, 2009.
[31] M. J. Bellman, R. J. Downey, A. Parikh, and W. E. Dixon, "Automatic control of cycling induced by functional electrical stimulation with electric motor assistance," *IEEE Trans. Autom. Science Eng.*, vol. 14, no. 2, pp. 1225–1234, April 2017.
[32] L. Marchal-Crespo and D. J. Reinkensmeyer, "Review of control strategies for robotic movement training after neurologic injury," *J. Neuroeng. Rehabil.*, vol. 6, no. 1, 2009.
[33] K. P. Tee, R. Yan, and H. Li, "Adaptive admittance control of a robot manipulator under task space constraint," in *IEEE Int. Conf. Robot. Autom.* IEEE, 2010, pp. 5181–5186.
[34] Y. Li and S. S. Ge, "Impedance learning for robots interacting with unknown environments," *IEEE Trans. Control Sys. Tech.*, vol. 22, no. 4, pp. 1422–1432, 2014.
[35] F. L. Lewis, "Nonlinear network structures for feedback control," *Asian J. Control*, vol. 1, no. 4, pp. 205–228, 1999.
[36] F. L. Lewis, R. Selmic, and J. Campos, *Neuro-Fuzzy Control of Industrial Systems with Actuator Nonlinearities*. Philadelphia, PA, USA: Society for Industrial and Applied Mathematics, 2002.
[37] W. E. Dixon, A. Behal, D. M. Dawson, and S. Nagarkatti, *Nonlinear Control of Engineering Systems: A Lyapunov-Based Approach*. Birkhauser: Boston, 2003.
[38] R. Kamalapurkar, J. A. Rosenfeld, A. Parikh, A. R. Teel, and W. E. Dixon, "Invariance-like results for nonautonomous switched systems," *IEEE Trans. Autom. Control*, vol. 64, no. 2, pp. 614–627, Feb. 2019.
[39] F. H. Clarke, *Optimization and nonsmooth analysis*. SIAM, 1990.
[40] A. F. Filippov, "Differential equations with discontinuous right-hand side," in *Fifteen papers on differential equations*, ser. American Mathematical Society Translations - Series 2. American Mathematical Society, 1964, vol. 42, pp. 199–231.